International Journal of Heat and Mass Transfer 66 (2013) 939–947

Contents lists available at SciVerse ScienceDirect

International Journal of Heat and Mass Transfer

journal homepage: www.elsevier.com/locate/ijhmt

Numerical and experimental studies on laminar hydrodynamic and thermal characteristics in fractal-like microchannel networks. Part B: Investigations on the performances of pressure drop and heat transfer

Chun-ping Zhang [a,b], Yi-fu Lian [b], Xiang-fei Yu [a], Wei Liu [a,c], Jyh-tong Teng [b,*], Ting-ting Xu [a], Cheng-Hsing Hsu [b], Yaw-Jen Chang [b], Ralph Greif [d]

[a] School of Energy and Power Engineering, Huazhong University of Science and Technology, Wuhan 430074, PR China
[b] Department of Mechanical Engineering, Chung Yuan Christian University, Chungli 32023, Taiwan
[c] Wuhan University of Technology, China Wuhan, 430074, PR China
[d] Department of Mechanical Engineering, University of California at Berkeley, CA 94720, USA

ARTICLE INFO

Article history:
Available online 2 August 2013

Keywords:
Fractal-like microchannel
Pressure drop
Heat transfer
Coefficient of performance

ABSTRACT

In the present paper, the numerical simulations and experiments were carried out to explore the laminar hydrodynamic and thermal characteristics in the symmetrical fractal-like microchannel networks, and the pressure drop and heat transfer for the networks were compared with those for the S-shape and straight microchannels. To evaluate the comprehensive performances of the microchannels used in this study, the coefficients of performance were introduced based on two criteria. The influences of geometrical parameters of aspect ratio, branching level, and bend type on the behaviors of flow and heat transfer were investigated in detail. The studies showed that parameters of both aspect ratio and branching level had substantial effects on the pressure drop and heat transfer. In addition, the bends with fillets in the microchannels were verified to reduce the local pressure loss compared with those having 90° bends. However, the fillet had little contribution to the heat transfer. It was concluded that a microchannel network with a smaller aspect ratio, a higher branching level, and a fillet bend would achieve a higher performance associated with pressure drop and heat transfer.

1. Introduction

In the companion paper [1] of the present article, the related studies [2–12] were reviewed in detail. Thus, the present article will not provide reviews of these studies again to avoid redundancy. From the research conducted in [1], it was concluded that the friction factors obtained by using the subsectional integral method were much higher than those obtained by using the conventional equivalent method; on the contrary, the Nusselt numbers obtained from the subsectional integral method were much lower than those obtained from the conventional equivalent method. As a result, compared with the experimental results, the deviations of the Reynolds number and the Nusselt number obtained from the conventional equivalent method were larger than those-obtained from the subsectional integral method. Moreover, at the bifurcations and bends, the secondary flow and recirculation flow motions were initiated, which made the developing flow region (1) regenerate again after the bifurcations and bends and (2) maintain along the subsequent straight channel until reaching the next bifurcation or bend. Consequently, due to the developing flow effect, the friction factor was expressed in terms of the apparent friction factor [13].

To provide an in-depth study on the performance enhancement brought up by the configurations of the fractal-like microchannel networks, the following work associated with the flow and heat transfer characteristics needs to be implemented. Firstly, although some research has been done on the fractal-like or tree-like microchannel networks as presented by [6–12], the configuration designs are all different as a result of their specific applications. For example, in order to have a free circulation of the cooling fluid and a uniform heat transfer, the test section was designed to be composed of two microchannel networks, which resulted in more pressure loss [6,7]. In addition, due to the fact that the costs of the wafer material and of manufacturing the test chip were high, a single microchannel network with a symmetrical fractal-like configuration on one silicon plate was designed. Moreover, performance evaluations and optimizations presented in most research were conducted on the branching level numbers of microchannels with a constant aspect ratio [7–10]. However, the heat transfer efficiency was also influenced by the aspect ratio as demonstrated by Soupremanien et al. [14]. Besides, the shape of the bends

* Corresponding author. Tel.: +886 3 2654308; fax: +886 3 2654399.
E-mail address: tengcycu@hotmail.com (J.-t. Teng).

0017-9310/$ - see front matter © 2013 Elsevier Ltd. All rights reserved.
http://dx.doi.org/10.1016/j.ijheatmasstransfer.2013.07.021

Nomenclature

A_c	cross sectional area
A_p	total plenum cross sectional area
c_p	specific heat at constant pressure
COP	coefficient of performance
D_h	hydraulic diameter
D_L	fractal dimension associated with microchannel length
D_d	fractal dimension associated with microchannel diameter
f	friction factor
f_{app}	apparent friction factor
H	microchannel height
h'	heat transfer coefficient
k_c	contraction loss coefficient
k_e	expansion loss coefficient
k_{90}	loss coefficient at the 90° bend
k_{tee}	loss coefficient at the Tee
L	microchannel length
$\dot{m}$	mass flow rate
N	branch number
P_w	wetted perimeter
ΔP	pressure loss
$\dot{Q}$	heat transfer rate
Re	Reynolds number
T	temperature
ΔT	temperature difference
u	velocity
$\dot{V}$	volume flow rate
W	microchannel width

Greek symbols

α	aspect ratio
β, γ	ratio of fractal dimension
λ	thermal conductivity
μ	dynamic viscosity
ρ	density

Subscripts

i	inlet
i, j	indices in Einstein summation convention
m	arithmetic mean
max, min	maximal and minimal value
m, log	log mean temperature difference
n	level number
o	outlet
w	channel wall being heated

affected the pressure drop and the heat transfer [15]. In another study [16], the fractal-like microchannels with two branching levels and three aspect ratios had been studied preliminarily; thus, as a further investigation in the present study, the performances of the fractal-like microchannel networks were compared among those networks with aspect ratios, branching levels, and bends. Subsequently, comparisons of the coefficients of performance obtained from the currently developed fractal-like microchannel networks with those obtained from the existing S-shape and straight microchannels were conducted. Furthermore, from the previous results shown in [1], the hydrodynamically and thermally developing flow effects were taken into account for all the fractal-like microchannel networks and the apparent friction factor was used rather than using the fanning friction factor [13].

2. Configuration design of the fractal-like microchannel network

The fractal-like network branching resulted in an increased number of channels with a smaller diameter and a rise in the total cross sectional flow area, which helped improve the efficiency of mass and momentum transfers. However, the enhancement of the efficiencies due to the branching levels and aspect ratios exist limitations as far as the pressure drop and heat transfer were concerned. Since the general shape of a micro-electronic chip was rectangular, the branching angle was often set to be 180° [17], and every channel was divided into two branches at the next level. The ratios of the lengths and diameters of the channels at the $(n+1)$th branching level to that at the nth branching level are characterized by the following scaling laws [18,19]:

$$\gamma = \frac{L_{n+1}}{L_n} = N^{-1/D_L} \tag{1}$$

$$\beta = \frac{D_{h(n+1)}}{D_{hn}} = N^{-1/D_d} \tag{2}$$

where L_n and D_{hn} represent the length of the microchannel segment and the hydraulic diameter at level n, respectively, and n is indexed from zero. N represents the number of branches, which is equal to two. D_L and D_d are fractal dimensions associated with the length and diameter of the microchannels, respectively, which is equal to three according to Murray's law of minimizing the network flow resistance for a fixed total microchannel volume [20]. However, by taking the value of 3 at higher branching levels for the length scale factor D_L, it will result in an overly dense and overlapped microchannel network. In the present configuration design, if the fractal dimension D_L was larger than 1, then the overlap would happen at the 5th level; thus, for geometric reasons and further study, $D_L = 1$ was adopted.

To generate a fractal-like microchannel network as shown in Fig. 1(a), a length L_0 and a diameter D_{h0} at the zeroth level are given; the relationship between the various branching lengths are characterized as follows:

$$L_{na} = L_{nb} \tag{3}$$

$$\frac{L_{(n+1)a} + L_{(n+1)b}}{L_{na} + L_{nb}} = N^{-1/D_L} \tag{4}$$

And the hydraulic diameter at the entrance is given by:

$$D_{h0} = \frac{4A_{c0}}{P_{w0}} \tag{5}$$

where A_{c0} is the cross sectional area of the channel and P_{w0} is the wetted perimeter at the zeroth level. Then the hydraulic diameter and the cross sectional area at the nth level are:

$$\frac{D_{hn}}{D_{h0}} = \frac{1+\alpha_0}{1+\alpha_n} \tag{6}$$

$$\frac{A_{cn}}{A_{c0}} = \frac{\alpha_n}{\alpha_0} \tag{7}$$

where α is the aspect ratio of a channel, $\alpha = H/W$, and H and W are the width and height of a channel, respectively. The branching levels of the fractal-like microchannel network were chosen to be one and two as shown in Fig. 1(b) and (c), respectively. The height for all channels being tested was 125 μm, with the maximum percentage

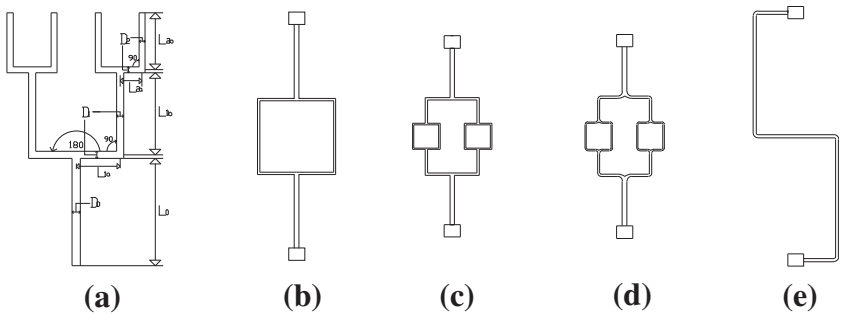

Fig. 1. Schematic diagram of microchannel models: (a) definition of a fractal-like microchannel network model, (b) a microchannel network with one branching level and 90° bends, (c) a microchannel network with two branching levels and fillet bends, (d) a microchannel network with two branching levels and fillet bends, (e) S-shape microchannel with fillet bends.

uncertainty being 5%. Such channels were in the range (10 μm < smallest dimension <200 μm [13]) considered to be microchannels. The widths were 125, 250, and 375 μm, corresponding to the aspect ratios of 1, 0.5, and 0.333, respectively, for three kinds of fractal-like microchannel networks. The channel length was 4000 μm at the zeroth level, 2000 μm at the 1st level, and 1000 μm at the 2nd level. Furthermore, to compare the pressure loss and heat transfer, the fractal-like microchannel networks and the S-shape microchannels were designed to have fillets at all the bends, as shown in Fig. 1(d) and (e). Finally, the behaviors of pressure drop and heat transfer for flow through all microchannels used in this study were compared with those through the straight microchannels, based on the same surface area for heat transfer. The classifications of microchannels used in the present work are given in Table 1.

The microchannel configurations with different geometric parameters were fabricated in silicon wafers with a diameter of 4 in. (10.16 mm) and a thickness of 550 μm using standard micro-electro-mechanical technologies. The processes included a SiO_2 deposition, a photoresist coating and developing, an oxide removing, and a baking, etc. as shown in Fig. 2. To ensure that a configuration of rectangular in cross-section and a high aspect ratio were achievable for the microchannels under study, the inductively coupled plasma-reactive ion etching (ICP-RIE) process accounting for the crystal directional characteristics was chosen to finish the etching of the microchannel structures. To quantify the surface roughness of the microchannels, a profilometer (made by Mitaka, Model NH-3 N) and a scanning electron microscope (SEM) were used to measure the surface profile of the microchannels. It was concluded from the measured results that since the peak-valley roughness of the silicon microchannel was lower than 70 nm, 0.056% of the shortest length of the microchannels, the wall surface of the microchannels was treated as smooth enough to neglect the slip behavior [21,22]. Subsequently, the inlet and outlet of the cover of microchannels were fabricated by applying the excimer laser to drill two holes on the thermal insulation glass (made by Pyrex 7740 with a thickness of 550 μm). Prior to the drilling, the thermal insulation glass was anodically bonded with the silicon wafer underneath to enclose the microchannel. This made the assembled test chip ready for the observations of the flow patterns. In addition, the sealing of the microchannel test chip prevented the microstructure in the test section from being influenced by its environment.

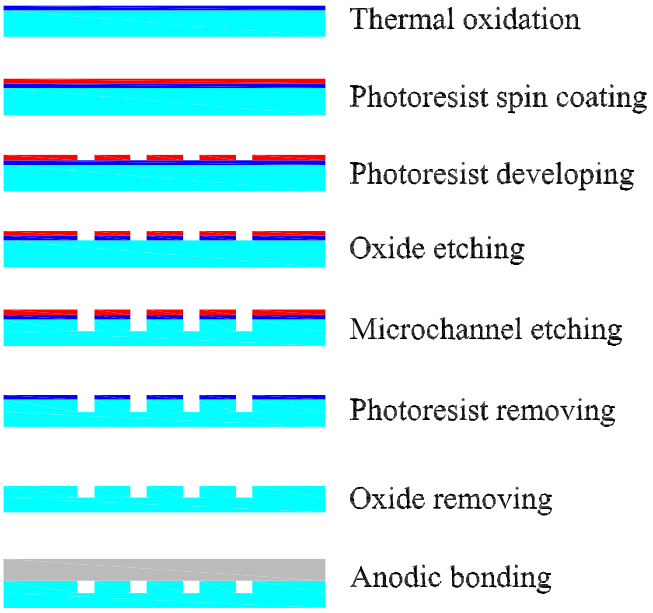

Fig. 2. Flow chart of the fabrication process of the fractal-like microchannel network.

3. Numerical analysis

In order to compare with the experimental results, the numerical simulations were performed using the commercial software package of CFD-ACE + 2006, based on the finite volume method (FVM). The broadly used steady three-dimensional governing equations for the laminar and Newton incompressible flow are listed as follows.

For the continuity equation:

$$\frac{\partial}{\partial x_i}(\rho u_i) = 0 \tag{8}$$

Table 1
Classifications of the microchannels.

Aspect ratio	One branching level	Two branching levels	Two branching levels with fillet bends	S shape	Straight shape
1	125-1	125-2	125-2 C	125-S	125-0
0.5	250-1	250-2	250-2 C	250-S	250-0
0.333	375-1	375-2	375-2 C	375-S	375-0

For the momentum equation:

$$\frac{\partial}{\partial x_i}(\rho u_i u_j) = \frac{\partial}{\partial x_i}\left(\mu \frac{\partial u_j}{\partial x_i}\right) - \frac{\partial P}{\partial x_j} \tag{9}$$

For the energy equation:

$$\frac{\partial}{\partial x_i}(\rho u_i T) = \frac{\partial}{\partial x_i}\left(\frac{\lambda}{C_p}\frac{\partial T}{\partial x_i}\right) + \frac{\mu}{C_p}\left(\frac{\partial u_i}{\partial x_j} + \frac{\partial u_j}{\partial x_i}\right)\frac{\partial u_i}{\partial x_j} \tag{10}$$

where i and j are indices in Einstein summation convention, u_i and u_j are the velocity components, P is the pressure, ρ and μ are the fluid density and dynamic viscosity, respectively. Apart from the governing equations, the related boundary conditions are provided as follows:

(1) Inlet: The initial temperature of the working fluid and the ambient air temperature are maintained at 297 K.
(2) Outlet: The ambient pressure is used as the reference pressure of the fluid at the outlet.
(3) Interface: The interfacial condition at solid/liquid interface requires continuities in temperatures and temperature gradients.
(4) Wall: The upper wall of the microchannel is treated as adiabatic, while the other three sides of the channel walls are maintained at a constant wall temperature of 323 K.

Based on the above mathematic formulations and boundary conditions, one half of the fractal-like microchannel networks was chosen to be the computational domain due to the geometric symmetry. To achieve the stability of solution convergence, the second-order upwind discretization scheme was used to perform the computation and the SIMPLE algorithm was employed for the pressure–velocity coupling. The convergence criterion was set to be 10^{-6}, and the iteration number was 2000. After comparing the running time and errors of the trial cases with grid numbers of 120,000, 260,000, 500,000, 630,000, and 870,000, the grid number of 500,000 was finally chosen for all cases under study.

The experimental setup and measurement process could be found in [1]. Both the hydrodynamic and thermal analyses were conducted in the developing flow region since the characteristic lengths of L_h and L_t for the flow to become fully-developed were all longer than those of the branching channel. And the subsectional integral method developed in [1] was adopted to numerically compute the parameters of flow and heat transfer. It is noted that, for the S-shape and straight microchannels, the entry region of hydrodynamics is a small fraction of the channel length; thus, it is appropriate to use the assumption for fully developed flow.

3.1. Pressure drop

For the experimental system as a whole, the measured pressure drops include the frictional pressure drop and the losses at the entrance, the bends, and the exit in the microchannels. Thus the overall measured pressure drop is the sum of these components [23]:

$$\Delta P = \frac{\rho u_m^2}{2}\left[\frac{4 f_{app} L}{D_h} + K_c + K_e + 2(A_c/A_p)^2 K_{90} + K_{tee}\right] \tag{11}$$

where ρ is the density of the fluid, u_m is the average flow velocity of the fluid, and f_{app} is the apparent frictional factor, accounting for the pressure drop due to the friction and the developing region effects. L is the length of the channel, K_c and K_e represent the contraction and expansion loss coefficients due to area changes, A_c and A_p are the total channel area and the total plenum cross sectional area, K_{90} is the loss coefficient at the 90° bend, and K_{tee} is the loss coefficient at the tee.

3.2. Heat transfer

When fluid flows through the microchannels, the heat $\dot{Q}$ removed by the fluid can be expressed by

$$\dot{Q} = \dot{m} c_p (T_0 - T_i) \tag{12}$$

where $\dot{m}$ represents the mass flow rate, c_p is the specific heat of the fluid, and T_i and T_0 are the temperatures of the working fluid at the inlet and outlet, respectively.

The heat transfer process in the present experiment includes the heat conduction from the brass plate to the silicon microchannel wall, and the heat convection from the microchannel wall to the working fluid. Due to the fact that the thermal conductivities associated with the silicon and brass are high (resulting in a minimal thermal resistance between them), no thermal loss between the silicon wall and the brass plate is assumed. Therefore the heat coming from the brass plate is equal to the heat transferred to the working fluid, and the heat transfer coefficient h' is the overall heat transfer coefficient. From Newton's law of cooling, the average heat transfer coefficient h' is calculated by

$$h' = \frac{\dot{Q}}{A_w \Delta T_{m,\log}} \tag{13}$$

where $\Delta T_{m,\log}$, the log mean temperature difference, is defined by

$$\Delta T_{m,\log} = \frac{\Delta T_{\max} - \Delta T_{\min}}{\ln\left(\frac{\Delta T_{\max}}{\Delta T_{\min}}\right)} \tag{14}$$

where $\Delta T_{\max} = T_w - T_i$, $\Delta T_{\min} = T_w - T_o$, and T_w is the average channel wall temperature. A_w is the area of the channel wall over which heat is added. Since the microchannels were covered with a Pyrex 7740 plate by a thin layer of adhesive, the upper wall was considered to be adiabatic and the other three sides were maintained at the constant wall temperature. For a fractal-like microchannel network, the total area heated in the channel is the sum of all the heated branching channel areas:

$$A_w = \sum_{i=0}^{n} A_{wi} \tag{15}$$

For each branching channel, the area A_{wi} is:

$$A_{wi} = 2W_0 L_0 + 4L_0 H + 2n \cdot \sum_{i=0}^{n}\left[4L_0\gamma^i + W_i^2 + \mathrm{H}\left(8L_0\gamma^i + 2W_i - W_{i-1}\right)\right] \tag{16}$$

where n is the level number, W_0 and L_0 are the width and length of the channel at the zeroth level, respectively. The branching channel width W_i is:

$$W_i = \frac{W_0 H \beta^i}{\left(W_0 + H - W_0\beta^i\right)} \tag{17}$$

Hence, the Nusselt number can be deduced from its definition and the average heat transfer coefficient h':

$$Nu' = \frac{h' D_h}{\lambda_m} = \frac{\dot{m} c_p D_h}{\lambda_m A_w} \ln\frac{\Delta T_{\max}}{\Delta T_{\min}} \tag{18}$$

It should be noted that the physical properties (density ρ, dynamic viscosity μ, specific heat c_p, and thermal conductivity λ_m) for the working fluid specified above are determined, based on the mean temperature: $T_m = (T_i + T_0)/2$.

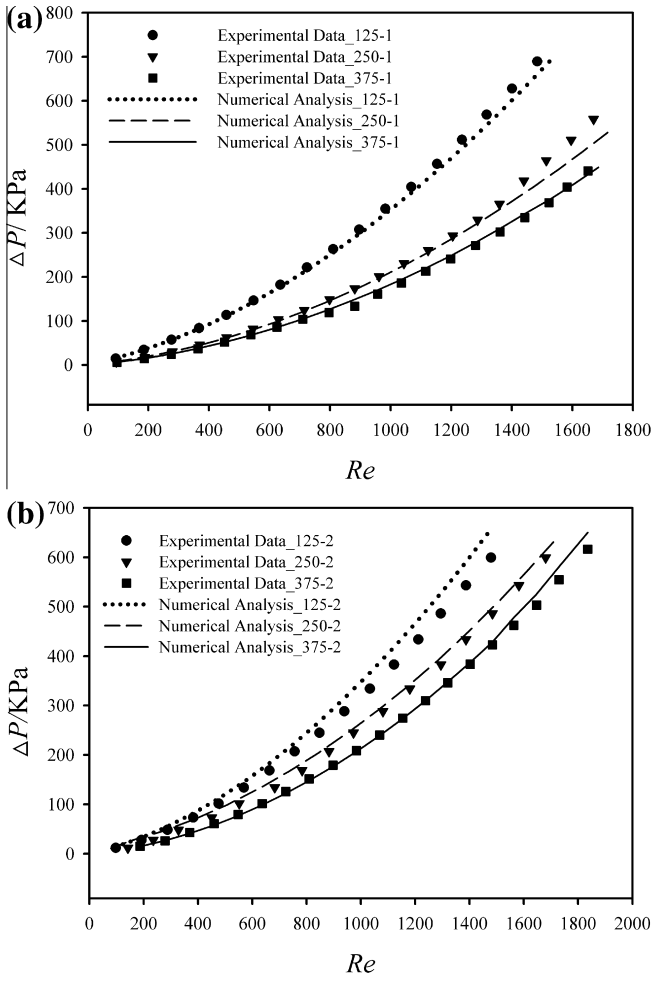

Fig. 3. Numerical and experimental pressure drops of the fractal-like microchannel networks with (a) one branching level and (b) two branching levels.

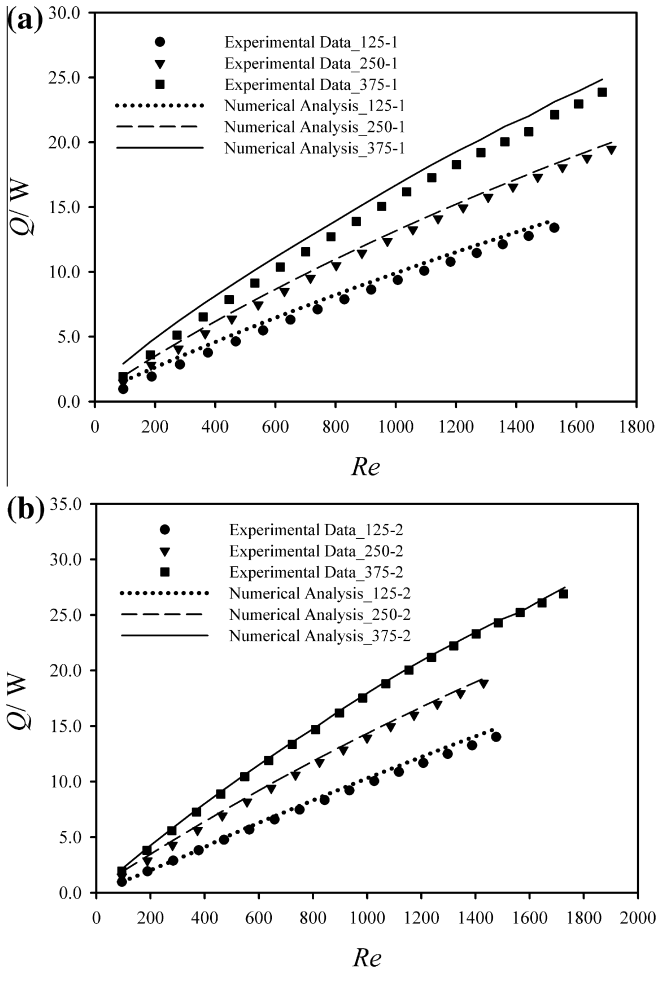

Fig. 4. Numerical and experimental heat transfer of the fractal-like microchannel networks with (a) one branching level and (b) two branching levels.

4. Results and discussion

4.1. Effects of the aspect ratios on the flow and heat transfer

The comparisons of the pressure drops obtained experimentally with those obtained numerically for the fractal-like microchannel networks with different aspect ratios are shown in Fig. 3(a) and (b). The results indicate fair qualitative influences of the Reynolds number and the aspect ratio on the hydrodynamic characteristics. The numerical results follow the same patterns and agree well with the experimental data. As can be seen from the curves, for both one and two branching levels, the pressure drops increase with the Reynolds numbers. Although the friction factor increases with a decrease in the aspect ratio as shown in Part A [1], the hydraulic diameter increases too. Thus, a larger aspect ratio results in a higher total pressure drop at a rapidly increasing rate. For the fractal-like microchannel network with two branching levels, the experimental pressure drop with the aspect ratio of 1 is 600 kPa at the Reynolds number of 1470, while by contrast, the pressure drops decrease by 29.7% and 19% corresponding to the channels with the aspect ratios of 0.333 and 0.5, respectively.

The experimental data and numerically calculated results of the heat transfer in the fractal-like microchannel networks are shown in Fig. 4. Similar to the change of the pressure drop, the heat transfer increases monotonously with an increase of the Reynolds number for two kinds of branching levels. But contrary to the pressure drop, the smaller the aspect ratio is, the larger the heat transfer becomes, due to the large contact area. When the Reynolds number is 1470, the experimental heat transfer in the microchannel networks with two branching levels are 24.31, 19.39, and 13.97 W, respectively, for the aspect ratios of 0.333, 0.5 and 1, which are increased by 74% and 38.8%, respectively, compared with that of the microchannel network with the aspect ratio of 1. Moreover, it is noticed that with an increase in the Reynolds number beyond 600, the effect of a smaller aspect ratio on the heat transfer becomes more pronounced.

4.2. Effects of the branching levels on the flow and heat transfer

For the same aspect ratio, the effects of the branching levels on the pressure drop obtained from the experimental results are seen from Fig. 5. In the figure, the behaviors of flow and heat transfer for the S-shape and straight microchannels are compared with those for the fractal-like microchannel networks of various branching levels with and without fillets at the bends. Since the high branching level produces more local pressure loss induced by the bifurcations and bends, the total pressure drops including the main and minor pressure losses with two branching levels go up more quickly with an increase in the Reynolds number than those with one branching level. When the Reynolds number is 1400 and the aspect ratio is 0.333, the pressure drops are 382.67, 274.76, 317.64, 249.27, and 154.07 kPa, respectively, for the microchannels with two branching levels without and with fillets, one branching

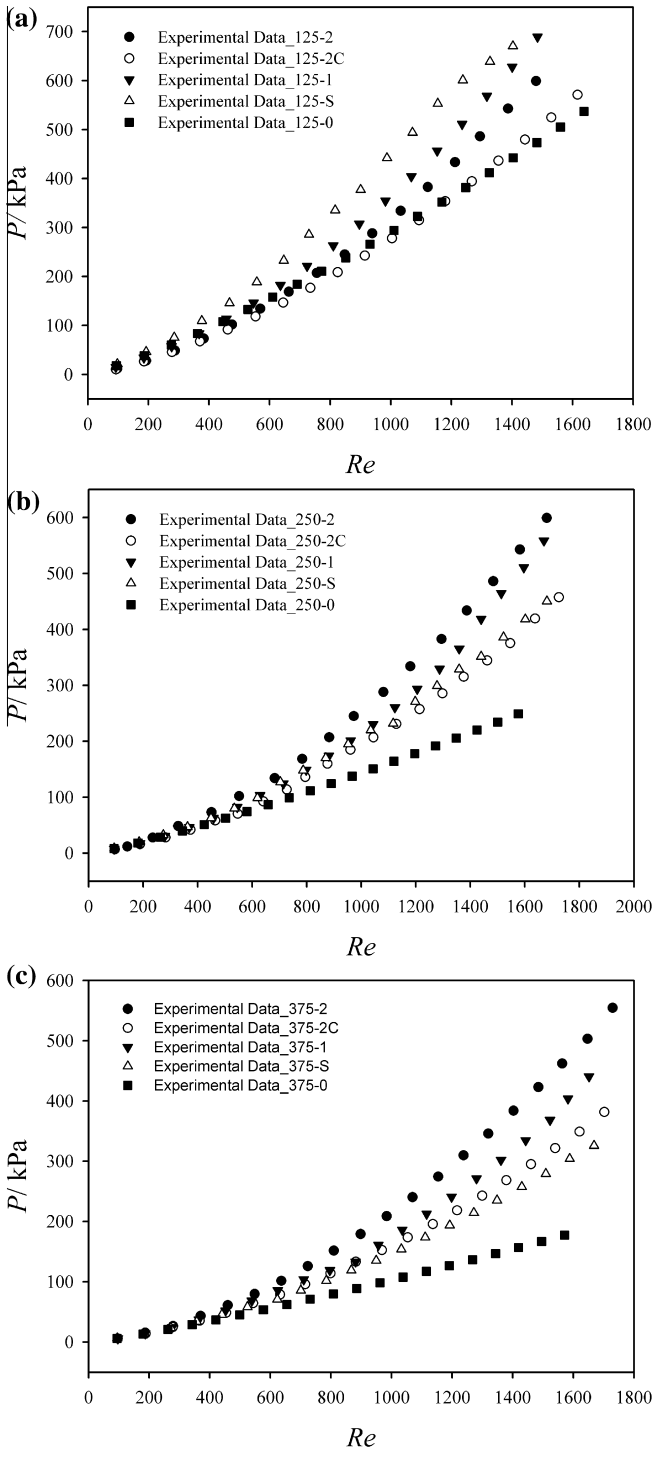

Fig. 5. Experimentally obtained pressure drops for different microchannels: (a) aspect ratio of 1, (b) aspect ratio of 0.5 and (c) aspect ratio of 0.333.

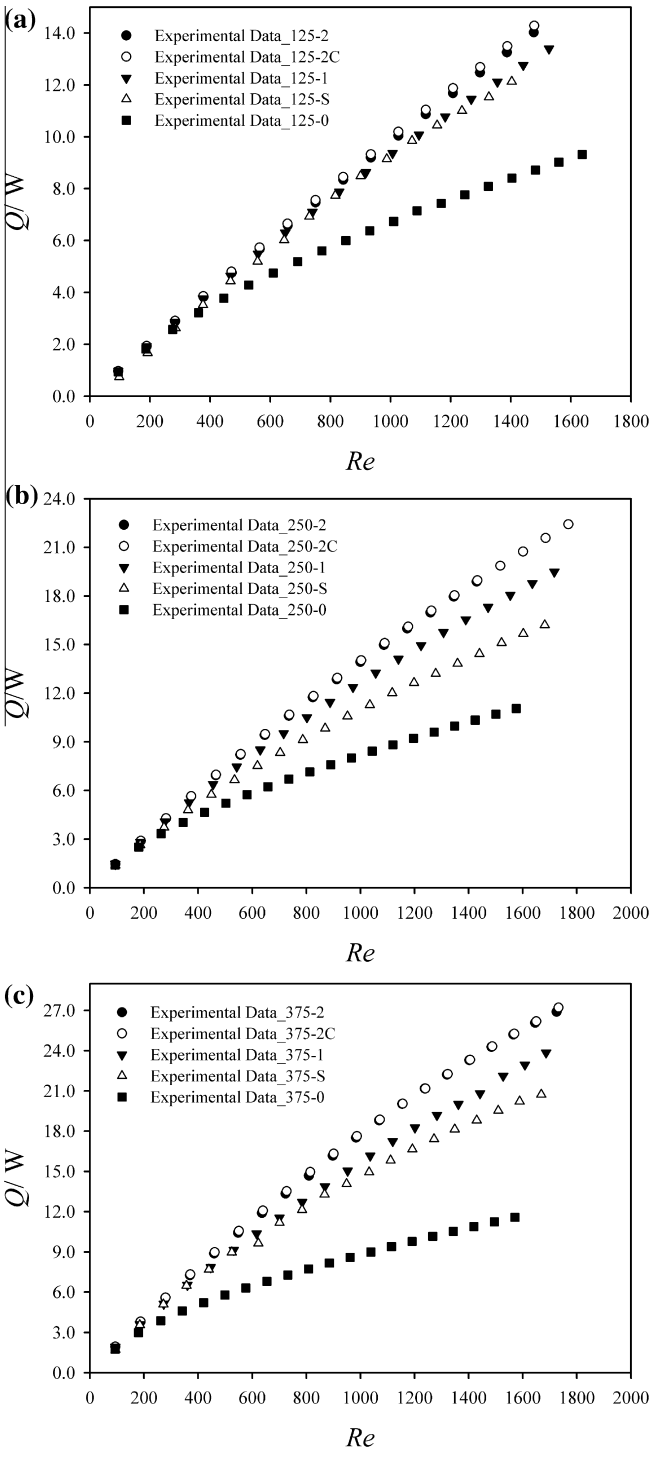

Fig. 6. Experimentally obtained heat transfer for different microchannels: (a) aspect ratio of 1, (b) aspect ratio of 0.5 and (c) aspect ratio of 0.333.

level, S-shape, and straight channels. In addition, at the Reynolds number of 1400 and for fractal-like microchannel networks with two branching levels, the bends with fillets for three aspect ratios of 1, 0.5, and 0.333 reduce the pressure losses of 16.9%, 26.6%, and 28.2%, respectively, compared with those with 90° bends. It is noted that for straight microchannels with three aspect ratios considered, as a result of the relatively small local pressure losses, the overall pressure drops take the lowest values among all the microchannels being studied, and at the same Reynolds number these values decrease as the aspect ratio decreases.

Furthermore, it is noted that when the aspect ratio is 1, the pressure drop of S-shape microchannel exceeds those of all other microchannels. But when the aspect ratio becomes smaller, the pressure drops of S-shape microchannels reduce gradually and fall behind those of the others, except those of the straight microchannels, as shown in Fig. 5(b) and (c). The constraint of the same heat transfer area used for comparison is the main reason contributing to this phenomenon for the S-shape microchannel, since the S-shape microchannel has the longest channel length among all microchannels considered for the case with the aspect ratio of 1.

However, with a decrease in the aspect ratio, the hydraulic diameter increases and the channel length becomes short for the S-shape microchannel, resulting in a gradually decreasing overall pressure drop.

The number of levels for the microchannel has a pronounced impact on the heat transfer performance, as shown in Fig. 6(a)–(c). Because the bifurcations disturb the flow in the streamwise direction and make the fluid enter the developing flow region again, the heat transferred in the fractal-like microchannel network with two branching levels is higher than that of all other microchannels being evaluated in this study. Furthermore, the secondary and recirculation flows associated with the velocity and temperature fields are generated at the bifurcations and bends of the fractal-like microchannel network, making the fluid being mixed to be more uniformly than those in the S-shape and straight microchannels. As a result, more heat is taken away by the fluid and the capability of the heat transfer is improved greatly in the fractal-like microchannel network with two branching levels, as shown in Table 2. Compared with the heat transfer from straight microchannels, the heat transfer from fractal-like microchannel networks with two branching levels increases by 61.9%, 82.4%, and 124%, respectively, corresponding to microchannels with aspect ratios of 1, 0.5, and 0.333. Moreover, it is seen that the effect of the aspect ratio on heat transfer in the fractal-like microchannel networks is larger than that of the straight microchannels; however, for fractal-like microchannel networks, the effect of the bends with fillets on the heat transfer in the networks is minimal relative to that on the pressure drop.

It is noted that all the experimental data used in this paper are averages of four measuring results. For pressure drop and heat transfer, the deviations between the numerical results and experimental data are within 7.2% and 6%, respectively, using the latter as the bases for comparison.

4.3. Coefficients of performance for the fractal-like microchannel networks

It is noted that the fractal-like microchannel network with a larger branching level and a smaller aspect ratio has an improved heat transfer capability; however, the pressure loss resulted from the presence of bifurcations and bends increases too. In general, both the pressure drop and the heat transfer increase with an increase in the Reynolds number. Therefore, it is necessary to use a comprehensive index to evaluate the overall performance. The coefficient of performance (*COP*) reflecting the general heat transfer performance at the expense of the pumping power is chosen and is expressed as [7,9]:

$$COP = \frac{\dot{Q}}{\Delta P \dot{V}} \tag{19}$$

where $\dot{V}$ is the volumetric flow rate. In view of the aspect ratios and branching levels have different influences on the pressure drops and heat transfer, the single *COP* of each kind of microchannel can not reflect its real performance under different situations. Thus, for further practical application, two dimensionless indexes of *COP* are introduced to get a general evaluation. The $COP/COP_{\alpha=1}$ is based on the coefficient of performance of the fractal-like microchannel networks with aspect ratio $\alpha = 1$ as shown in Fig. 7. And the COP/COP_0 is based on the coefficient of performance of straight channels with different aspect ratios, as shown in Fig. 8.

The curves of the $COP/COP_{\alpha=1}$ fall steeply in the low Reynolds number region and become flat in the high Reynolds number region after. Because of the contribution in the reduction of pressure loss, the $COP/COP_{\alpha=1}$ of the microchannels having bends with fillets are higher than those with 90° bends, and the differences of $COP/COP_{\alpha=1}$ between the microchannels with these two types of bends increase with an increase in the Reynolds number. It is noted that the fractal-like microchannel network with aspect ratio of 0.333 and bends with fillets has the highest value of $COP/COP_{\alpha=1}$. In addition, the$COP/COP_{\alpha=1}$ falls slightly with an increase in the number of branching levels since the fractal-like microchannel network with more branching levels results in higher pressure loss.

For the microchannels used in this study, the variations of the COP/COP_0 do not change monotonously with the Reynolds number. They increase in the region of low Reynolds number and decrease in the region of high Reynolds number, as shown in Fig. 8. And the smaller the aspect ratio is, the higher the amplitude of the fluctuation becomes. At the same Reynolds number, variations in the rates of increase in the pressure drop and the heat transfer are the main reason affecting the fluctuation. Therefore, to obtain a

Table 2
Experimentally obtained heat transfer for different microchannels tested at the Reynolds number of 1400.

Aspect ratio	Two branching levels with 90° bends (W)	Two branching levels with fillet bends (W)	One branching level with 90° bends (W)	S-shape with 90° bends (W)	Straight (W)
1	13.6	13.4	12.5	12.1	8.4
0.5	18.6	18.6	16.7	14.1	10.2
0.333	23.3	23.3	20.3	18.6	10.4

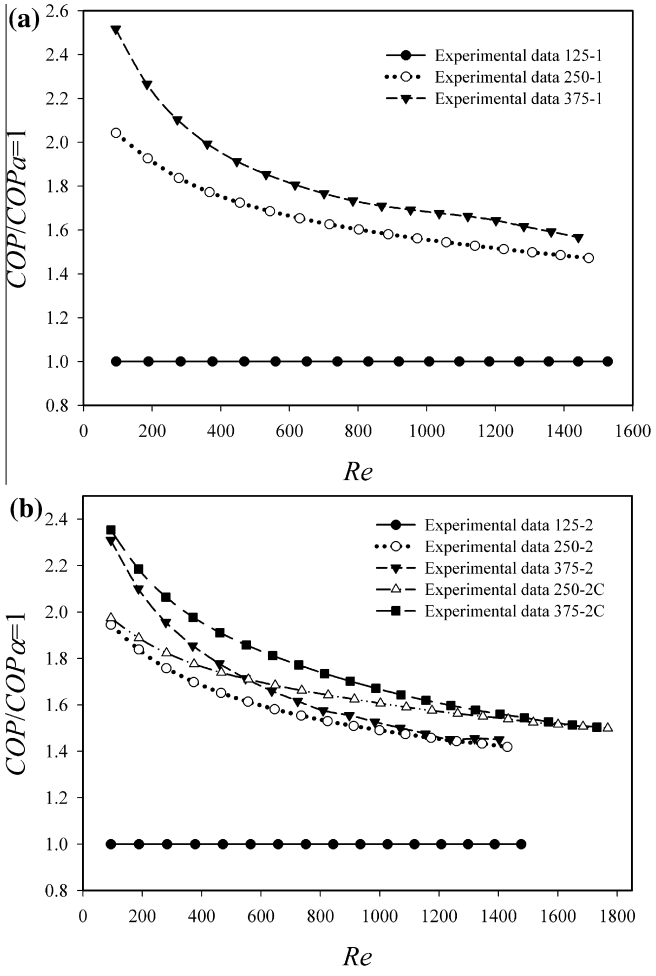

Fig. 7. Comparison of coefficients of performance for two types of fractal-like microchannel networks: (a) channels with one branching level and (b) channels with two branching levels.

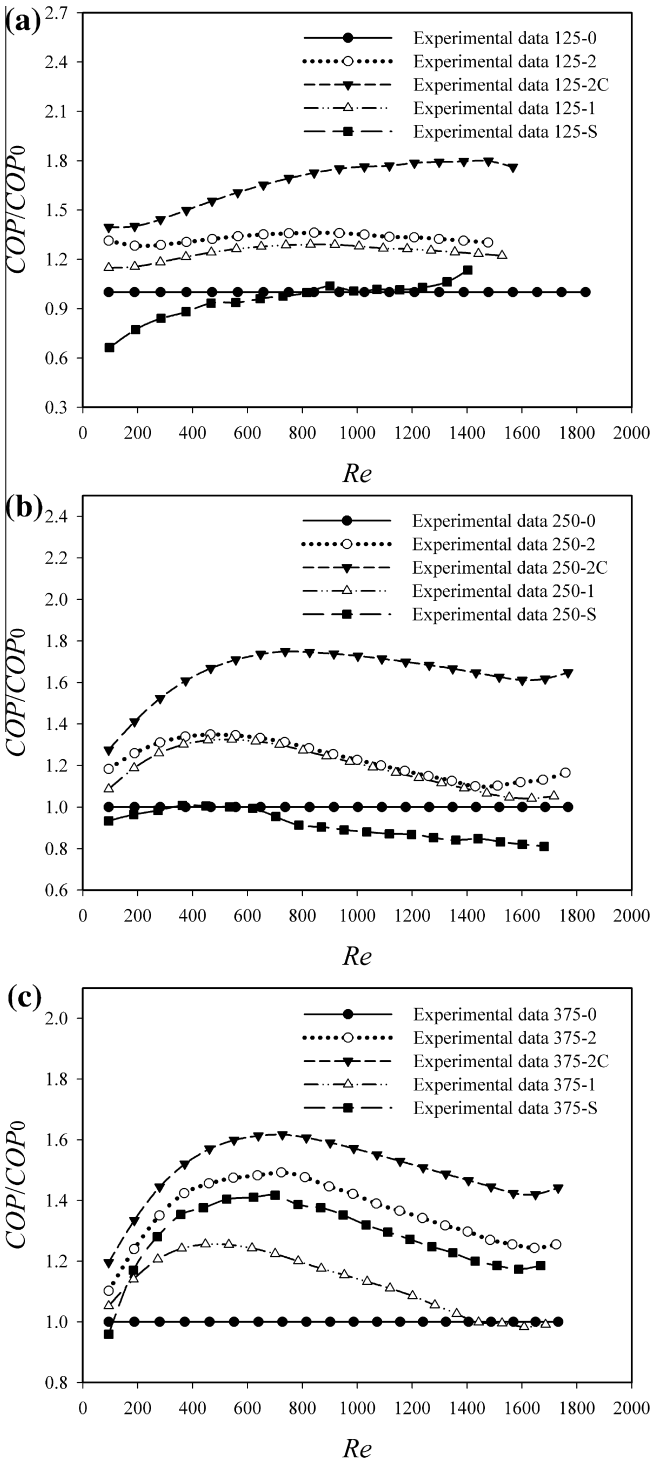

Fig. 8. Comparison of coefficients of performance for three kinds of microchannels: (a) channels with aspect ratio of 1, (b) channels with aspect ratio of 0.5 and (c) channels with aspect ratio of 0.333.

high coefficient of performance, both the branching levels and aspect ratios (together with the volumetric flow rates) need to be evaluated accounting for the pressure drop and heat transfer. The relative performance of the fractal-like microchannel network with fillet bends and two branching levels is the highest among all the microchannels under study. Although the performance of S-shape microchannel with an aspect ratio $\alpha = 0.333$ is higher than those of the fractal-like microchannel network with one branching level and the straight microchannel, for higher aspect ratio, its performance is even lower than that of the straight microchannel. These results correspond well with the behaviors of the microchannels as far as the pressure drop and the heat transfer are concerned.

5. Conclusions

The fractal-like microchannel networks with different branching levels and aspect ratios have been fabricated and investigated for the study on the behaviors of pressure drop and heat transfer, compared with those of the S-shape and straight microchannels. Then two indexes of the coefficient of performance were proposed and compared for the microchannels being studied. The results were presented as conclusions here:

(1) Both the aspect ratio and the branching level had substantial effects on the hydrodynamic and thermal characteristics of the fractal-like microchannel networks. It was shown by the results obtained from experimental data and those from numerical analyses that a larger aspect ratio resulted in a higher total pressure drop and a smaller heat transfer. Furthermore, due to the existence of bifurcations and bends in the fractal-like microchannel networks, a high branching level produced a high pressure drop and a large heat transfer, compared with the other microchannels. However, the bends with fillets for the fractal-like microchannel reduced the local minor pressure losses, compared with that with the 90° bends, resulting in a lower overall pressure drop.

(2) Comparison of results for the relative coefficient of performance $COP/COP_{\alpha=1}$ showed that at the same branching level, the fractal-like microchannel network with a smaller aspect ratio had a high coefficient of performance. While at the same aspect ratio, although the relative coefficient of performances COP/COP_0 for all microchannels had nonlinear relationships with the Reynolds number, the coefficients of performance for the fractal-like microchannel networks with two branching levels and bands with fillets were the highest.

In summary, from this study it was concluded that for a complex configuration such as a fractal-like microchannel network, besides the hydraulic diameter, the branching level and the aspect ratio were the dominant parameters affecting the pressure drop and heat transfer performances. The relative coefficient of performance has shown to be an effective index to evaluate the overall performance of the fractal-like microchannel networks.

Acknowledgments

The support of this work offered by the National Science Council, Taiwan, ROC, under contract Nos. NSC 99-2221-E-033-025 and NSC 100-2221-E-033-065, is gratefully acknowledged. The fabrication work of the tested microchannels by Material & Chemical Research Laboratories at Industrial Technology Research Institute in Hsin-chu, Taiwan is deeply appreciated.

References

[1] C.P. Zhang, Y.F. Lian, X.F. Yu, W. Liu, J.T. Teng, T.T. Xu, C.H. Hsu, Y.J. Chang, R. Greif. Numerical and experimental studies on laminar hydrodynamic and thermal characteristics in fractal-like microchannel networks. Part A: comparisons of two numerical analysis methods on friction factor and Nusselt number, Int. J. Heat Mass Transfer, 2013, in press.
[2] D.B. Tuckerman, R.F.W. Pease, High-performance heat sinking for VLSI, IEEE Electron Device Lett. 2 (1981) 126–127.
[3] A. Bejan, Constructal-theory network of conducting paths for cooling a heat generating volume, Int. J. Heat Mass Transfer 40 (1997) 799–815.
[4] A. Bejan, Design with Constructal Theory, Wiley, Hoboken, 2008.

[5] D.V. Pence, Reduced pumping power and wall temperature in microchannel heat sinks with fractal-like branching channel networks, Microscale Therm. Eng. 6 (2002) 319–330.
[6] Y.P. Chen, P. Cheng, Heat transfer and pressure drop in fractal tree-like microchannel nets, Int. J. Heat Mass Transfer 45 (2002) 2643–2648.
[7] Y.P. Chen, P. Cheng, An experimental investigation on the thermal efficiency of fractal tree-like microchannel nets, Int. J. Heat Mass Transfer 32 (2005) 931–938.
[8] X.Q. Wang, A.S. Mujumdar, C. Yap, Thermal characteristics of tree-shaped microchannel nets for cooling of a rectangular heat sink, Int. J. Therm. Sci. 45 (2006) 1103–1112.
[9] W. Escher, B. Michel, D. Poulikakos, Efficiency of optimized bifurcating tree-like and parallel microchannel networks in the cooling of electronics, Int. J. Heat Mass Transfer 52 (2009) 1421–1430.
[10] D. Heymann, D.V. Pence, V. Narayanan, Optimization of fractal-like branching microchannel heat sinks for single-phase flows, Int. J. Therm. Sci. 49 (2010) 1383–1393.
[11] B.J. Daniels, J.A. Liburdy, D.V. Pence, Experimental studies of adiabatic flow boiling in fractal-like branching microchannels, Exp. Therm. Fluid Sci. 35 (2011) 1–10.
[12] C. Zhang, Y. Chen, Flow boiling in constructal tree-shaped minichannel network, Int. J. Heat Mass Transfer 54 (2011) 202–209.
[13] S.G. Kandlikar, S. Garimella, D.Q. Li, S. Colin, M.R. King, Heat Transfer and Fluid Flow in Minichannels and Microchannels, Elsevier limited, Oxford, 2006.
[14] U. Soupremanien, S.L. Person, M.F. Marinet, Y. Bultel, Influence of the aspect ratio on boiling flows in rectangular mini-channels, Exp. Therm. Fluid Sci. 35 (2011) 797–809.
[15] D. Haller, P. Woias, N. Kockmann, Simulation and experimental investigation of pressure loss and heat transfer in microchannel networks containing bends and T-junctions, Int. J. Heat Mass Transfer 52 (2009) 2678–2689.
[16] X.F. Yu, C.P. Zhang, J.T. Teng, S.Y. Huang, S.P. Jin, Y.F. Lian, C.H. Cheng, T.T. Xu, J.C. Chu, Y.J. Chang, T. Dang, R. Greif, A study on the hydraulic and thermal characteristics in fractal tree-like microchannels by numerical and experimental methods, Int. J. Heat Mass Transfer 55 (2012) 7499–7507.
[17] X.Q. Wang, A.S. Mujumdar, C. Yap, Effect of bifurcation angle in tree-shaped microchannel networks, J. Appl. Phys. 102 (2007). 073530:1-8.
[18] G.B. West, J.H. Brown, B.J. Enquist, A general model for the origin of algometric scaling laws in biology, Science 276 (1997) 122–126.
[19] D.V. Pence, Improved thermal efficiency and temperature uniformity using fractal-like branching channel networks, in: Proceedings of the Engineering Foundation International Conference on Heat Transfer Transport Phenomena in Microscale, Banff, Canada, 2000, pp. 142–148.
[20] C.D. Murray, The physiological principle of minimum work: I. The vascular system and the cost of blood volume, Proc. National Acad. Sci. USA 12 (1926) 207–214.
[21] N.V. Priezjev, S.M. Troian, Influence of periodic wall roughness on the slip behavior at liquid/solid interfaces: molecular versus continuum predictions, J. Fluid Mech. 554 (2006) 25–46.
[22] X.Q. Wang, C. Yap, A.S. Mujumdar, Effects of two-dimensional roughness in flow in microchannels, J. Electron. Packag. 27 (2005) 357–361.
[23] P.S. Lee, S.V. Garimella, D. Liu, Thermally developing flow and heat transfer in rectangular microchannels of different aspect ratios, Int. J. Heat Mass Transfer 49 (2006) 3060–3067.